J. Chem. Eng. Data **2004,** *49,* 306−310

Evaluating the Thermodynamic Consistency of Experimental Data for HF + H_2O at 101.325 kPa

Christina M. Smith and Donald P. Visco, Jr.*

Department of Chemical Engineering, Tennessee Technological University, Box 5013,
Cookeville, Tennessee 38505

In this work we examine the thermodynamic consistency of the solution property data presented from three literature sources for a mixture of hydrogen fluoride and water at 101.325 kPa. The current work utilizes the Direct Test that allows for a discrete analysis of the experimental data rather than a conclusion on the data set as a whole. By using a three-parameter Margules equation along with an equation of state for determining vapor-phase fugacity coefficients, we find that at above 60% HF the experimental data become increasingly inconsistent. Additionally, we utilize Barker's method along with temperature-dependent Margules equation parameters to report model-predicted vapor-phase compositions that offer a compromise among the three experimental data sets. Discussion on this work relative to recent simulation results for this system is provided.

Introduction

A well-designed process is the backbone of profitability in the chemical process industry. Accurate thermophysical data are necessary to properly complete the design process; however, these data are not always readily available from experimentation, especially for certain systems that are difficult to work with. Such is the case for any mixture that contains the notoriously dangerous compound, hydrogen fluoride (HF).

Hydrogen fluoride has many industrial applications in both the aqueous and anhydrous forms. Anhydrous HF is mainly used as the source of fluorine ions in the production of fluorocarbons. Some fluorocarbon products include refrigerants, foam-blowing agents, seals, and coatings.[1] Other primary applications of anhydrous HF include fluorine ion derivative production, catalysis, and cleaning agents. Recently, the industrial demand for HF has increased as a result of replacing chlorofluorocarbons (CFCs) with hydrochlorofluorocarbons (HCFCs) and hydrofluorocarbons (HFCs). Hydrogen fluoride is also widely used in the aqueous form. Aqueous HF mixtures are used in the pickling of stainless steel as well as in the frosting and etching of glass.[2] Also, high purity aqueous HF mixtures are used in the etching of silicon wafers in semiconductor manufacturing.

Given the industrial importance of HF, knowledge of the physical properties of both anhydrous and aqueous HF is necessary. However, experimentation with HF involves many difficulties and dangers. Hydrogen fluoride is a toxic and corrosive substance, though it is normally classified as a weak acid. The difficulties associated with HF experimentation are mainly safety issues regarding exposure. Short-term exposure to HF causes severe burns, nausea, chest pains, pulmonary edema, and even death. Repeated or long-term exposure can lead to the development of a crippling disease known as fluorosis, in which one's bone density increases due to the collection of fluoride ions in the bone. Aqueous HF is less toxic than anhydrous HF; however, because it is a liquid, it is more difficult to handle and more corrosive. The reaction of HF with some metals also results in the production of hydrogen gas. Such experimental dangers hinder the acquisition of experimental data.

Experimental studies of aqueous HF are sparse in comparison to the number of studies for anhydrous HF. Munter et al.[3] published an early vapor−liquid equilibrium data set in 1947 for aqueous HF. Munter's work determined vapor−liquid equilibrium properties of this system including boiling points and compositions over a 5−89 HF mass % range at atmospheric pressure. Later, Vieweg[4] published experimental data for the same system over a broader range of pressure but for HF concentrations < 80 mass %. More recently, Miki et al.[5] published vapor−liquid equilibrium data for the aqueous HF system at 101.325 kPa utilizing a conductivity method they developed to precisely measure phase equilibrium over a 6.1−99.99995 HF vapor mol % range. Such high-concentration regions for HF in an aqueous mixture find utility in the promotion of technologies using dehydration of HF.

This work will examine the thermodynamic consistency of the three aqueous HF data sets above using the Gibbs−Duhem equation. Unlike Miki, we will not assume an ideal vapor phase when determining experimental activity coefficients but will model the nonidealities in the vapor by including fugacity coefficients obtained using a modified version of the association + equation of state (AEOS) model.[6] Gibbs excess energy models will be used to correlate the experimental data in order to evaluate thermodynamic consistency. Though not required, one can choose to incorporate the increasing strength of the acid at more-concentrated HF levels. However, debate exists across the composition region on the type of complexes present.[18] Since this is very much an open question, the modeling done in this work assumes no dissociation. Additionally, we utilize Barker's method [7] to predict vapor-phase compositions from a Gibbs excess energy model at various pressures. Finally, a discussion on the results of this work

---

* To whom correspondence should be addressed. E-mail: dvisco@tntech.edu. Phone: (931) 372−3606. Fax: (931) 372−6352.

10.1021/je034154g CCC: $27.50

relative to recent simulation results for this system is provided.

Thermodynamic Consistency

A recent study[8] was performed analyzing the thermodynamic consistency of the Miki data set using the Gibbs−Duhem integral test.[9] In that study, the vapor-phase fugacity coefficients were calculated using a version of the SAFT (SAFT-Variable Range or SAFT-VR).[10] Their integral test gave results that were an order of magnitude larger than the heuristic value used to evaluate thermodynamic consistency, even with the inclusion of a model for the vapor-phase nonidealities. However, their conclusion was not a definitive statement on the experimental data but an indictment of the predictive power of SAFT for this application.[8]

Though the integral test provides a necessary condition for thermodynamic consistency, it is not a sufficient condition. Additionally, it is a conclusion on the data set taken as a whole rather than on individual measurements. A more fruitful approach is the so-called "Direct Test" of thermodynamic consistency that allows analysis of each data point relative to the Gibbs−Duhem equation.[11] Here, one minimizes the sum of the squares of the residuals of the excess Gibbs energy and evaluates the residuals of $\ln(\gamma_1/\gamma_2)$, denoted $\delta \ln(\gamma_1/\gamma_2)$. Note that γ is the activity coefficient with subscripts 1 and 2 indicating HF and water, respectively. To the extent that $\delta \ln(\gamma_1/\gamma_2)$ differs from zero, one can draw conclusions as to the thermodynamic consistency of such an experimental data point.

Vapor-Phase Models

To obtain useful activity coefficients for the HF + H_2O system at 101.325 kPa, a model for the vapor phase must be chosen that adequately describes the nonidealities in that phase. The experimental compressibility factor (Z) for the pure components at 101.325 kPa is 0.98 for water[9] and 0.29 for hydrogen fluoride.[12] Thus, the ideal gas model that Miki used in his analysis does not account for the nonidealities present as the vapor becomes HF-rich. As previously mentioned, Juwono utilized SAFT-VR to determine the vapor-phase fugacity coefficients for this system. However, and as he recognized, his parametrization of such a model for an HF + water mixture was not adequate for a variety of system properties including a prediction of $Z = 0.998$ for saturated HF vapor at 101.325 kPa. Note that a recent reparametrization of SAFT-VR for hydrogen fluoride[13] improves the representation of the vapor phase but still predicts a compressibility factor of 0.63 for the saturated vapor at this pressure.

Recently, a modified version of an association + equation of state (AEOS) model to describe hydrogen fluoride was proposed and various mixtures, including HF + water, were explored using this model. Since this is the model utilized in the current study to account for vapor-phase nonidealities, we will provide some background information on this approach.

The AEOS model for hydrogen fluoride separates the association contributions (here called "chemical") to the compressibility factor from those of the other system interactions (here called "physical"), such that $Z = Z^{ch} + Z^{ph} - 1$. Note that "ch" should be read as chemical while "ph" should be read as physical. The formation of oligomer species from the monomer is modeled as self-association chemical reactions. The values for the equilibrium constants of these self-association reactions are given relative to a dimerization equilibrium constant through a Poisson-like distribution function. This distribution accounts for one parameter while the dimerization constant accounts for three parameters.

The chemical part of the compressibility factor is given exactly as a ratio of infinite sums, but the sums are both functions of Z^{ch} and, hence, require iteration to be solved. However, Anderko showed that Z^{ch} can be written in terms of a reduced density (q) and subsequently solved for Z^{ch} over a range of values for q. Next, he proposed a functional form that fit the exact values for Z^{ch}, allowing this model to be utilized without iteration, making it useful for process analysis. Subsequent work by one of us improved on this functional fit, allowing the heat effects to be modeled more accurately.[14] This functional form contains eight parameters.

Finally, the physical part of the compressibility factor is modeled by the Peng−Robinson equation of state. Here, four adjustable parameters are used (three for the energy parameter and a temperature-independent size parameter).

When using the AEOS model for the system under study in this work, we have assumed that water behaves as a nonassociating inert compound. In the vapor this is, at first glance, a reasonable assumption, as pure water exhibits limited association in the vapor relative to HF. Thus, water is parametrized only through its Peng−Robinson parameters (here, two for the energy parameter and one for the temperature-independent size parameter). Finally, a binary interaction parameter is utilized to reproduce the experimental azeotrope at 101.325 kPa.

When using this model for the saturated HF vapor at 101.325 kPa, a value of 0.28 is predicted for the compressibility factor that is in very good agreement with the experimental value of 0.29. Accordingly, we have used the AEOS-predicted vapor-phase fugacity coefficients for the HF + water system in calculating the experimental activity coefficients in this work. Note that we have not enforced phase equilibrium requirements on the AEOS model. Rather, we used the experimental temperature, pressure, and vapor-phase composition as inputs to the AEOS model with the fugacity coefficient as the output. We do this in order to use all of the experimental data available. The fugacity coefficient values for the vapor from the AEOS model are reported in Table 1 and presented graphically in Figure 1.

It is clear from Table 1 and Figure 1 that the AEOS model treats this system as behaving nonideally in the vapor phase. As required, values for the fugacity coefficient in the mixture approach that at saturation near the composition end points. However, the model predicts complex behavior for the fugacity coefficient of water in the concentrated HF region with values above 3. One can speculate that such a number indicates, perhaps, a strange repulsion-dominated interaction where HF molecules exclude and isolate water molecules so as not to mitigate any HF self-association interactions.

Excess Gibbs Energy Modeling

After various Margules equations as well as the Wilson equation were explored, it was determined that a three-parameter Margules equation was a reasonable description of this system without overfitting. Specifically, the three-parameter Margules equation is given as[15]

$$\frac{G^E}{RTx_1x_2} = A_{21}x_1 + A_{12}x_2 - C_{21}x_1x_2 \tag{1}$$

where G^E is the excess Gibbs energy, x is the liquid-phase

Table 1. Vapor-Phase Fugacity Coefficients from the AEOS Model and the Activity Coefficients Calculated Using These Fugacity Coefficients[a]

x_{HF}	y_{HF}	T (°C)	ϕ_{HF}^{sat}	$\hat{\phi}_{HF}$	ϕ_{water}^{sat}	$\hat{\phi}_{water}$	γ_{HF}	γ_{water}
				Munter et al.				
0.091	0.018	102.8	0.5885	0.9937	0.9907	1.0085	0.0302	0.9996
0.184	0.064	106.6	0.5897	0.9902	0.9898	1.0081	0.0487	0.9340
0.278	0.178	110.3	0.5897	0.9831	0.9886	1.0077	0.0807	0.8118
0.474	0.783	106.2	0.5893	0.9398	0.9898	1.0100	0.2195	0.3411
0.678	0.987	65.5	0.5703	0.7842	0.9972	1.0487	0.4682	0.1718
0.793	0.992	44.9	0.5498	0.6521	0.9988	1.2525	0.6373	0.5045
0.879	0.994	33.3	0.5331	0.6039	0.9993	1.9185	0.7955	1.7656
				Vieweg				
0.0910	0.0181	102.8	0.5885	0.9936	0.9907	1.0085	0.0303	0.9995
0.1838	0.0615	106.6	0.5897	0.9904	0.9898	1.0081	0.0465	0.9369
0.2785	0.1768	110.3	0.5897	0.9831	0.9886	1.0077	0.0801	0.8131
0.3751	0.4096	111.7	0.5904	0.9690	0.9882	1.0076	0.1318	0.6445
0.4738	0.7220	106.2	0.5894	0.9437	0.9898	1.0095	0.2033	0.4362
0.5746	0.9009	87.0	0.5834	0.8892	0.9942	1.0178	0.3163	0.3864
0.6775	0.9859	65.5	0.5704	0.7843	0.9972	1.0486	0.4679	0.1818
0.7827	0.9990	47.6	0.5530	0.6677	0.9986	1.1978	0.6090	0.0511
				Miki et al.				
0.227	0.0609	108.5	0.5898	0.9907	0.9891	1.0080	0.0356	0.9212
0.395	0.4928	113.7	0.5907	0.9656	0.9875	1.0076	0.1435	0.5347
0.411	0.5853	113.2	0.5906	0.9599	0.9877	1.0079	0.1644	0.4571
0.520	0.9416	101.5	0.5883	0.9212	0.9910	1.0128	0.2637	0.1179
0.636	0.9949	76.0	0.5778	0.8374	0.9960	1.0300	0.3987	0.0366
0.720	0.9970	57.1	0.5632	0.7300	0.9980	1.0866	0.5338	0.0683
0.863	0.9989	35.5	0.5370	0.6140	0.9992	1.7521	0.7671	0.2490
0.908	0.99937	29.8	0.5274	0.5868	0.9994	2.2859	0.8543	0.3779
0.99382	0.999901	20.3	0.5098	0.5158	0.9996	3.4597	0.9830	2.3494
0.99735	0.999949	19.8	0.5100	0.5118	0.9996	3.5374	0.9956	2.9929
0.99933	0.999987	19.5	0.5094	0.5094	0.9996	3.5850	1.0006	2.8693
0.999951	0.99999907	19.5	0.5094	0.5094	0.9996	3.5852	1.0000	3.0610
0.999978	0.99999950	19.5	0.5094	0.5094	0.9996	3.5852	1.0000	3.6076

[a] The significant figures reported for the compositions come from the indicated literature sources.

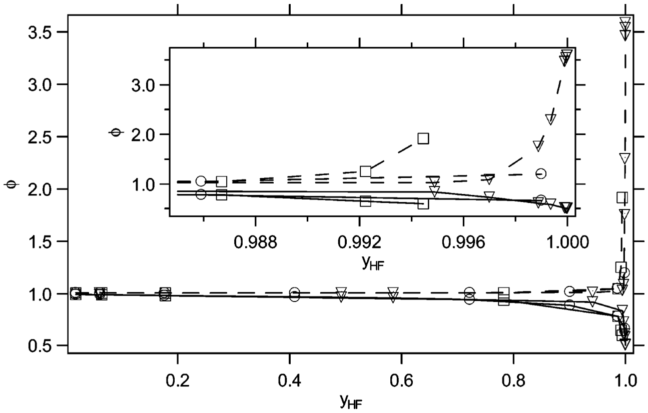

Figure 1. Mixture fugacity coefficients presented as a function HF mole fraction. The symbols are as follows: squares , Munter et al.;[3] circles, Vieweg;[4] inverted triangles, Miki et al.[5] Lines, drawn as guides for the eye, indicate species, with a solid line representing HF and a dashed line representing water.

Table 2. Parameters and Root Mean Square Errors for the Three-Parameter Margules Equation Model

parameter	value	parameter	value
A_{21}	−2.4964	C_{12}	14.1014
A_{12}	−1.4054	rms($\delta G^E/RT$)	0.1757
		rms($\delta \ln(\gamma_1/\gamma_2)$)	2.2074

mole fraction, R is the gas constant, T is the absolute temperature, and A_{21}, A_{12}, and C are fitting parameters. Since the three data sets studied are isobaric (101.325 kPa), the temperature varies as a function of composition. The three parameters were determined by minimizing the sum of the squares of the residuals in G^E/RT (see Table 2). The experimental values for the activity coefficients were calculated using

$$\gamma_i = \frac{y_i P \hat{\phi}_i}{x_i P_i^{\text{sat}} \phi_i^{\text{sat}}} \tag{2}$$

(the following are all for component i), where y_i is the vapor-phase mole fraction, $\hat{\phi}_i$ is the fugacity coefficient in the vapor mixture, ϕ_i^{sat} is the fugacity coefficient of the pure saturated vapor at the mixture temperature, and P_i^{sat} is the experimental saturated vapor pressure.

The experimental results for the activity coefficients are presented in Table 1 while in Figure 2 we show the residuals of G^E/RT and $\ln(\gamma_1/\gamma_2)$ plotted as a function of mole fraction. In the Miki et al. work where the vapor was considered an ideal gas, the infinite-dilution activity coefficient for water approached unity. However, by including nonidealities in the vapor in the manner described in this work, the infinite-dilution activity coefficient for water was ~3.6.

Table 2 provides the root-mean-square (rms) error for both residuals plotted in Figure 2. As required, the residuals of G^E/RT scatter about zero, but $\delta \ln(\gamma_1/\gamma_2)$ residuals do not, especially at mole fractions above 0.60 HF. Clearly the results from this test indicate inconsistency in the more-concentrated HF regions. Note that, according to the Consistency Index proposed by Van Ness[11] on the rms error of $\ln(\gamma_1/\gamma_2)$, this data set as a whole would score well below the lowest mark (index = 10), indicating data of very poor quality.

Barker's Method

At this point it is clear the AEOS-predicted vapor-phase fugacity coefficients imply that thermodynamic inconsis-

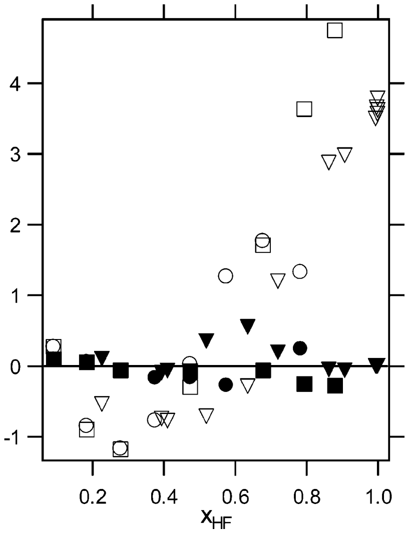

Figure 2. Residuals (defined as model − experiment) for G^E/RT and $\ln(\gamma_1/\gamma_2)$ presented as a function HF mole fraction. The filled symbols are for $\delta(G^E/RT)$ while the empty symbols are for $\delta\ \ln(\gamma_1/\gamma_2)$. The symbols are as follows: squares, Munter et al.;[3] circles, Vieweg;[4] inverted triangles, Miki et al.[5]

tency exists in the experimental data reported for this system at 101.325 kPa, especially at the more-concentrated HF region of composition space. Since temperature and liquid-phase mole fractions are most easily measured experimentally, relative to vapor-phase compositions, we can utilize the Gibbs−Duhem equation constraint to provide for mole fractions in the vapor.[15]

To account for the temperature dependence of the Margules equation parameters in the subsequent analysis, we write the parameters in eq 1 as

$$A_{21} = A_{210}/T + A_{211} - A_{212} \ln T \tag{3}$$

$$A_{12} = A_{120}/T + A_{121} - A_{122} \ln T \tag{4}$$

$$C_{21} = C_{210}/T + C_{211} - C_{212} \ln T \tag{5}$$

The excess enthalpy equation from the three-parameter Margules equation is[15]

$$\frac{H^E}{RTx_1x_2} = A'_{21}x_1 + A'_{12}x_2 - C'_{21}x_1x_2 \tag{6}$$

Using the enthalpy data of Tyner[16] at 20 °C and 100 °C for the HF/water system at 101.325 kPa, we are able to parametrize the relationship in eq 6, which, in turn, allows the evaluation A_{210}, A_{212}, A_{120}, A_{122}, C_{210}, and C_{212}. Then, the parameters A_{211}, A_{121}, and C_{211} are fit by minimizing the sum of the squares of the residuals in the temperature. To obtain vapor pressure values for the pure components at the required temperatures during iteration, an Antoine equation ($\ln P = A - B/(T + C)$; P/kPa; T/°C) was used to fit the experimental vapor pressure data over the temperature range of interest for this problem, which resulted in the following parameters: HF, $A = 17.3291$, $B = 4536.77$, $C = 337.467$; water, $A = 17.0532$, $B = 4299.21$, $C = 245.62$. The parameter values and the root mean square error from four residuals are shown in Table 3. Note that including the heat effects into the parametrization made the agreement with experiment worse (rms($\delta G^E/RT$) increased from 0.1757 to 0.3275 while rms($\delta\ \ln(\gamma_1/\gamma_2)$) increased from 2.2074 to 5.1796).

Table 3. Parameters and Root Mean Square Errors for the Three-Parameter Margules Equation (*T*-Dependent) Model

parameter	value	parameter	value
A_{210}	−18638.7785	C_{210}	−44241.6660
A_{211}	291.7404	C_{211}	872.4919
A_{212}	41.9079	C_{212}	126.7849
A_{120}	−7393.8700	rms($\delta G^E/RT$)	0.3275
A_{121}	93.2485	rms($\delta\ \ln(\gamma_1/\gamma_2)$)	5.1796
A_{122}	12.9819	rms(δT) (in K)	3.3305
		rms(δy)	0.0655

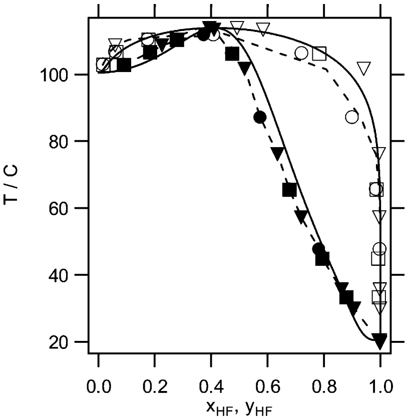

Figure 3. Bubble (filled symbols) and dew point (empty symbols) temperatures presented as a function of HF mole fraction at 101.325 kPa. Symbol types are as per Figure 1. The solid line is the AEOS prediction while the dashed line is the prediction from Barker's method using a temperature-dependent three-parameter Margules equation.

Figure 3 shows the results of this parameter fitting in the form of a *Txy* plot relative to experimental data. The vapor-phase compositions above around 40 mol % HF predicted from application of Barker's method offer somewhat of a compromise between all three experimental data sets. The AEOS model, which is an equation of state that can be used to obtain fugacity coefficients for both phases (and, hence, provide phase equilibrium predictions independent of any activity coefficients), is presented as well and provides qualitative agreement with experiment.

Conclusions

In this work, we analyzed the thermodynamic consistency of three aqueous HF data sets taken at 101.325 kPa using a three-parameter Margules equation. The Direct Test of thermodynamic consistency using this model indicated that data taken above 60 mol % HF are increasingly less consistent than data taken below that percentage. Additionally, vapor-phase compositions were predicted using Barker's method in conjunction with a temperature-dependent three-parameter Margules equation. The results of Barker's method indicate a compromise in the vapor-phase compositions among the three data sets.

While performing this research, an ongoing study evaluating the thermodynamic consistency of the aqueous HF system using molecular simulation came to our attention.[17] These authors use a biasing technique within the Monte Carlo simulation to determine the vapor-phase fugacity coefficients and, ultimately, perform an integral test on the experimental data. The simulation work paints a different picture of the behavior for the fugacity coefficients, especially in the dilute/concentrated regions. For example, while the AEOS model predicts the fugacity coefficient for water in the dilute water region to sharply rise to a value above 3, simulation predicts the opposite behavior, with a sharp decrease to near zero. Likewise, the AEOS model predicts the fugacity coefficient for HF in the dilute HF region to be ideal, while simulation predicts a value around 0.2. On the basis of these results for the fugacity coefficients, simulation finds that the experimental data do satisfy the integral test. However, it is to be noted (as the authors do) that simulation does not provide a complete picture of this system. For example, the simulation predicts the vapor-phase compressibility factor for HF to be 0.63 at 101.325 kPa, compared to the experimental value of 0.29. This latter property, on the other hand, is well-correlated by the AEOS model.

The combined efforts of thermodynamic modeling in this work and the briefly described results from simulation studies provide a nice compliment to each other and demonstrate the utility of a variety of approaches in an attempt to understand complex phenomena. While simulation is more time-consuming and more difficult to implement, it has provided evidence that thermodynamic models for the HF/water mixture should include water as an associating species in the vapor phase, despite the fact that it associates to a degree far less than that of HF if in a pure vapor. Accordingly, from the thermodynamic modeling end, we are currently developing a model that includes water association into the AEOS.

Acknowledgment

The author's are grateful for the comments and suggestions of the reviewers in improving the quality of this work. Additionally, work of Saravanan Swaminathan and Barath Baburao in calculating the fugacity coefficients is acknowledged.

Literature Cited

(1) Smith, R. A. *Kirk-Othmer Encyclopedia of Chemical Technology*; Wiley: New York, 1991; Vol. 11.
(2) Simons, J. H. In *Fluorine Chemistry*; Simons, J. H., Ed.; Academic Press: New York, 1950.
(3) Munter, P. A.; Aepli, O. T.; Kossatz, R. A. Hydrofluoric acid−water and hydrofluoric acid-hydrofluosilicic acid−water. *Ind. Eng. Chem.* **1947**, *39*, 427−431.
(4) Vieweg, R. Ein Enthalpie-Konzentrations-Diagramm des Systems Fluorwasserstroff-Wasser. *Chem. Technol. (Berlin)* **1963**, *15*, 734.
(5) Miki, N.; Maeno, M.; Maruhashi, K.; Ohmi, T. Vapor-liquid equilibrium of the binary system HF−H_2O extending to extremely anhydrous hydrogen fluoride. *J. Electrochem. Soc.* **1990**, *137*, 787−794.
(6) Baburao, B.; Visco, D. P. VLE/VLLE/LLE Predictions for hydrogen fluoride mixtures using an improved equation of state. *Ind. Eng. Chem. Res.* **2002**, *41*, 4863−4872.
(7) Prausnitz, J. M.; Lichtenthaler, R. N.; de Azevedo, E. G. *Molecular Thermodynamics of Fluid-Phase Equilibria*; Prentice Hall: Englewood Cliffs, NJ, 1986.
(8) Juwono, E. M. S. State University of New York at Buffalo, 1999.
(9) Smith, J. M.; Van Ness, H. C.; Abbott, M. M. *Introduction to Chemical Engineering Thermodynamics*, 5th ed.; McGraw-Hill: New York, 1996.
(10) Gil-Villegas, A.; Galindo, A.; Whitehead, P. J.; Mills, S. J.; Jackson, G.; Burgess, A. N. Statistical associating fluid theory for chain molecules with attractive potentials of variable range. *J. Chem. Phys.* **1997**, *106*, 4168−4186.
(11) Van Ness, H. C. Thermodynamics in the treatment of vapor/liquid equilibrium (VLE) data. *Pure Appl. Chem.* **1995**, *67*, 859−872.
(12) Kao, C.-P. C.; Paulaitis, M. E.; Sweany, G. A.; Yokozeki, M. An equation of state/chemical association model for fluorinated hydrocarbons and HF. *Fluid Phase Equilib.* **1995**, *108*, 27−46.
(13) Galindo, A.; Burton, S. J.; Jackson, G.; Visco, D. P.; Kofke, D. A. Improved models for the phase behaviour of hydrogen fluoride: chain and ring aggregates in the SAFT approach and the AEOS model. *Mol. Phys.* **2002**, *100*, 2241−2259.
(14) Visco, D. P.; Kofke, D. A. Improved Thermodynamic Equation of State for Hydrogen Fluoride. *Ind. Eng. Chem. Res.* **1999**, *38*, 4125−4129.
(15) Van Ness, H. C.; Abbott, M. M. *Classical Thermodynamics of Nonelectrolyte Solutions*, 1st ed.; McGraw-Hill Book Company: New York, 1982.
(16) Tyner, M. Enthalpy Concentration Diagram for Hydrogen-Fluoride Water System at One Atmosphere. *Chem. Eng. Prog.* **1949**, *45*, 49−52.
(17) Wierzchowski, S. J.; Kofke, D. A. Liquid-phase activity coefficients for saturate HF/H2O mixtures with vapor-phase nonidealites described by molecular simulation. *Ind. Eng. Chem. Res.* **2004**, *43*, 218−227.
(18) Sillanpaa, A. J.; Simon, C.; Klein, M. L.; Laasonen, K. Structural and Spectral Properties of Aqueous Hydrogen Fluoride Studied Using ab Initio Molecular Dynamics. *J. Phys. Chem. B* **2002**, *106*, 11315−11322.

Received for review August 8, 2003. Accepted December 20, 2003.

JE034154G